ISSN: 2449 - 0539
BAYERO JOURNAL OF ENGINEERING AND TECHNOLOGY VOL 17, NO. 3 AUG 2022 pp 53- 64

ESTIMATION OF DC SERVOMOTOR PARAMETERS USINGGREY WOLF, WHALE AND GENETIC ALGORITHM OPTIMISATION TECHNIQUES

Nyong-Bassey Bassey Etim[1*], Epemu Ayebatonye Marttyns[2]
[1,2]Department of Electrical/Electronic Engineering, Federal University of Petroleum Resources Effurun, Effurun, Nigeria.
[*]Corresponding author email: Nyongbassey.bassey@fupre.edu.ng

ABSTRACT

This paper investigates the use of time-domain response with recent meta-heuristic optimisation techniques such as; Grey wolf optimisation, Whale optimisation algorithm, and Genetic algorithm for the estimation of the parameters of a servomechanism with insufficient datasheet information. First, to estimate the servomechanism's closed-loop position second-order transfer function, the known servo gear mechanism and unknown speed first-order transfer functions were used. In the experimental investigation, the average time constant of the Servomechanism was found to be 162mS for both forward and reverse rotations. Thereafter, the meta-heuristic algorithms were used in MATLAB to simulate the identified position closed-loop velocity feedback transfer function to obtain the Servomechanism's electromechanical parameters. The simulation and experimental response of the servomechanism were in excellent agreement, with the Genetic and Whale optimisation algorithms having the best and worst root mean squared error fitness scores of 0.00706 and 1.90374 respectively.

Keywords: Systems Identification, Genetic Algorithm, Grey Wolf Optimization, Whale Optimization, Servomechanism

1. INTRODUCTION

A Servomechanism controls position and motion and consists of a minimum of one mechanical part. Furthermore, the principle of control is such that the control may be implemented in an open-loop or closed-loop configuration. The open-loop configuration usually consists of a proportional controller which affects the feed-forward loop when varied (Armstrong, 2015). The open-loop control is inadequate in tracking the output response as a high-gain results in overshoot and steady-state error. Also, the closed-loop control implementation is such that a negative feedback loop derived from the output response and the input reference demand are summed up to give an error signal. This error signal is then used to drive the servo mechanism input (Armstrong, 2015; Kabita, 2015).

According to Bartelt (2010), two branches of control exist Process control and Servomechanism. In process control, the reference input demand rarely gets altered rapidly for this reason the speed of tracking process variables such as temperature and pressure is typically slow. However, in servomechanism control, the set-point changes much more rapidly such that the system tracks the output variable as fast as possible, where such variables may include position and speed. Additionally, to enhance the transient response of the position servo control systems, a cascaded control loop consisting of the position and velocity feedback is used simultaneously. The effect of the velocity feedback is basically to dampen out the overshoot in the transient response and is analogous to derivative control action. More so, Bartelt (2010), asserts that the velocity feedback also provides for a better torque rejection hence, leading to a robust control configuration.

Nevertheless, it is desirable to identify the Servomechanism parameters from their transfer function, where they may be unknown or partially known in other to carry out analytical studies and establish the transfer function equation governing the control of the Servomechanism (Garrido and Miranda, 2012). Therefore, the Servomechanism parameters may be determined analytically using methods such as the step response time plot or the frequency domain Bode plot (Throne, 2005; Kabita, 2015). Nevertheless, the frequency response method is quite tedious and less intuitive compared to the time domain step response. Thus, by obtaining the time constant and DC steady-state gain of an open-loop step response, the transfer function of the system can be determined by comparing it with a classical first-order equation.

Furthermore, in Garrido and Concha (2010), the least square error (LSE) technique is utilised for parameter identification wherethe input excitation reference signal is usually of the rich frequency component. The authors (Kim and Chung, 2003; Fuh and Tsai, 2007) suggested the use of two biased input square wave signals for accurate parameter identification of a linear servomechanism. In the process of identifying the systems transfer function and estimated parameters, the input square wave biased signal was used and the corresponding output signal with the assumption that the DC servomechanism is a linear system.

More recently, artificial intelligencebased on nature-inspired meta-heuristic optimisation algorithms, such as genetic algorithm (GA) (Pan *et al.*, 2021), particle swarm optimisation (PSO) (Nyong-Bassey and Akinloye, 2014), Grey wolf optimisation (Mirjalili*et al*., 2014), whale optimisation algorithm (Mirjalili and Lewis, 2016), which do not use gradient techniques to solve complex mathematical and engineering problems (Mohamed *et al*., 2018).

Specifically, in (Chun and Kim, 2018) a novel hybridized particle swarm optimisation (PSO) algorithm was used to effectively demonstrate the simultaneous identification of both model structure and the associated parameters in a magnetic levitation system and a flexible robotic manipulator. Also, in Wu, *et al*., (2019) validation in MATLAB and ADAMS showed that control error and steady-state accuracy were improved by 75% and 50% with PSO and finite time servo system control used to estimate the systems physical parameters.

In Nadweh*et al*., (2020), the GWO had a better reduction in total harmonic distortion and ripple factor current in the DC link of a variable speed drive system for the estimated optimal controller parameter estimation

In Nayak and Sahu, (2019) the dc motor parameters were estimated using meta-heuristic whale algorithm optimisation (WOA) which mimics the bubble-net foraging process of humpback whales. The experimental data of the dc motor speed response was used to generate a reference model which was compared to an adaptive model tuned by minimising the error speed response between the models via three independent integral time square error fitness functions.

Furthermore, in Guo *et al*., (2022) a proposed WOA improved with a reverse learning strategy and the Levy flight disturbance strategy was used to accurately identify the parameters of a static var compensator model.

In Rezazade, (2010) GA and LSE were used to estimate the parameters of servo electrical drives. The GA compared to the LSE had better results in the start-up phase lacking persistent excitation.Salah and Omar (2019), estimated the parameters of a DC motor using an offline identification toolbox in MATLAB/Simulink based on experimental step response.

Similarly, in Fang et al, (2021) the use of an adaptive GA with a fractional-order UKF was proposed to improve state error caused by inaccurate parameter estimation of a lithium-ion battery model and state of charge respectively. Also, in Wu et al, (2020) WOA and UKF were combined for Battery model parameters and SOC estimation respectively.

While, the GA (Fang et al, 2021), GWO (Nadweh*et al*., (2020)), and more recently WOA (Guo *et al*., (2022),) have been usedindividually for parameter estimation,to the best of our knowledge fromavailable literature, GWO has not been used for DC servo motor parameter estimation. More so, the performance of all threeGA, WOA and GWO has never been compared simultaneouslyforparameter estimation of anexperimental modular MS150 DC servo motor-system.

Therefore, themain contribution of this paper is to comparatively investigate the unknown parameters of the MS150DC servo motor system, using the GA, WOA and particularly GWO technique for DC motor parameter estimation by adapting a simulation model in MATLAB software to the closed-loop position step response transfer function of a cascade servomechanism obtained from experimental data.

2. METHODOLOGY

The DC servo system under investigation is the modular MS150 designed by feedback instrumentswhich consistsof the DC servomotor; armature-controlled DC Motor, and servo amplifier DCM150F+SA150D, a tachometer GX150X withservo motor speed to angle converter system, oscilloscope and the pulse generator/power supply.

The experiment to determine the unknown parameters of the MS150 DC servo system was performed in the United Kingdom at Newcastle University's Electrical and Electronics Engineering Laboratory.

The MS150 experimental setup is implemented in the open-loop configuration. The input power supply to the system is -/+15V, while a pulse generator is used to excite the DC servo motor with a reference voltage signal (Vm)of range +/-3.0V. Thereafter, as a consequence of the (+/-) excitation voltage the DC servo motor SA150D+DC M150F, rotates in the clockwise and anticlockwise directions respectively.While the output speed of the motor in revolutions per minute and tachometer voltage is measured using the tachometer and the oscilloscope. Figure 1, shows the MS150 modular DC servo motor system.

ISSN: 2449 - 0539
BAYERO JOURNAL OF ENGINEERING AND TECHNOLOGY VOL 17, NO. 3 AUG 2022 pp 53- 64

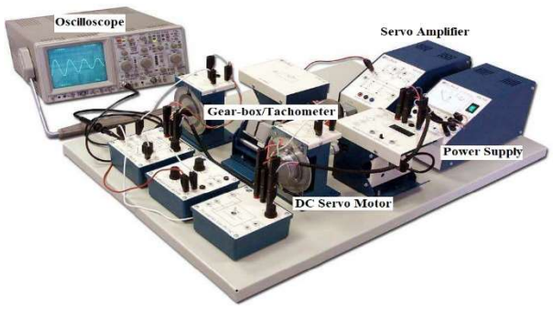

Figure 1: MS150 DC Servo modular system (Feedback Instruments, 2013)

2.1 Servo Motor Modelling

To mathematically model the DC servo motor, the simplified schematic diagram presented in Figure 2, is used. The modelling of the DC Servo motor involves the use of both Kirchhoff's voltage law and Newton's second law of motion to obtain the mathematical equations for the electrical armature coil winding and the mechanical rotor components respectively (Nyong-Bassey and Akinloye, 2014; Adewusi, 2016).

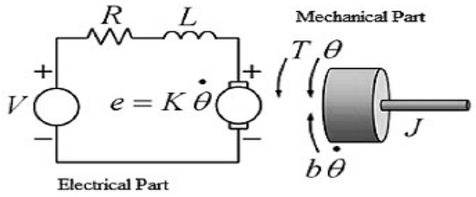

Figure 2: DC Servo motor

Thus, the electrical armature differential equations of the DC Servo motor are presented in (1) as follows:

$$\frac{di}{dt} = \frac{1}{L}(V - Ri - E)\ldots \quad (1)$$

Where L is the inductance of the armature coil winding (in Henry), R is the Resistance of the armature coil (in Ohms), E is the back E.M.F in the armature winding (in Volts), I is the current in the armature winding (in amperes), V is the voltage across the armature winding (in Volts).

The mechanical rotor equation is presented in (2) as follows:

$$\frac{di}{dt} = \frac{1}{J}(Ki - Bw)\ldots \quad (2)$$

Where,

$$E = K * w\ldots \quad (3)$$

$$K = Ke\ldots \quad (4)$$

$$T = Ke * i\ldots \quad (5)$$

T is mechanical torque (in Nm), J is the moment of inertia of the rotor (in Kgm-2), B is the motor's coefficient of friction (in Nm/(rad/sec)), K is Back E.M.F motor constant (Nm/A), ω is the angular velocity of the mechanical rotor (rad/sec), θ is the angular position of the mechanical rotor (rad).

The transfer function for the output speed and input voltage of the Servo motor is obtained by taking the Laplace transform of (1) and (2) is given below:

$$G(s) = \frac{\omega(s)}{V(s)} = \frac{K}{\{(JS+B)(LS+R)+K^2\}}\ldots \quad (6)$$

Also, by integrating speed, the position can be derived therefore, the position transfer function is as follows:

$$T(s) = \frac{\theta(s)}{V(s)} = \frac{K}{\{(JS+B)(LS+R)+K^2\}S}\ldots \quad (7)$$

2.2 Servo Motor Time Constant and gain

The servomotor transfer function $G(s)$ is based on a first-order system structure and is given by:

$$G(s) = \frac{\omega_m}{V_m} = \frac{K_m}{1+S\tau_m}\ldots \quad (8)$$

Where, ω_m is output angular velocity, V_m is servomotor excitation voltage, K_m is the servomotor gain constant and τ_m is an equivalent electro-mechanical time constant.

The servo gain can be determined in two ways:

$$K_m = \omega / Vm \quad \ldots(9)$$

Also, Servo gain may be determined by:

$$K_m = V_t/(V_m * K_t)\ldots (10)$$

Therefore, since the servo gear transfer function H(s) is known and coupled to the G(s), the position open-loop transfer function is $\boldsymbol{T_{OL}}$ (s):

$$\boldsymbol{T_{OL}(s)} = \frac{K_m}{1+S\tau_m} * H(s)\ldots(11)$$

Where,

$$H(s) = 6.65/s \quad \ldots(12)$$

2.3 Meta heuristic Optimisation Algorithms

This section describes the fundamental principles of the nature-inspired meta-heuristic algorithms; GWO, and WOA which are based on swarm intelligence and GA which is based on evolution.

2.3.1 Grey wolf optimization

The grey wolf optimiser (GWO) which is based on meta-heuristics is a recent and novel type of swarm intelligence optimisation algorithm, first introduced in (Mirjalili*et al.*, 2014; Wang and Li, 2019). The fundamental principles of the GWOare based on the hunting behaviour and the social hierarchy of grey. To obtain an optimal solution, the grey wolf hunts prey using three steps; encircling, hunting and attacking while adhering strictly to the social hierarchy

of leadership. Therefore, the social hierarchy from top to bottom consists of four groups of wolfs; the alpha (α), beta (β) delta (δ) and omega (ϖ). Thus, excluding the omega wolf, each wolf group is followed by their subordinate wolf groups. For instance, the alpha wolf leads the rest of the wolf groups i.e. beta, delta and omega, while, the beta wolf leads the delta and omega wolfs. Hence, the alpha wolf guides the pack during hunting while the beta, delta and omega follow accordingly. Consequently, the pack's movement is dictated by the three best solutions termed alpha beta and delta respectively with less optimal solutions considered omega wolves (Kushwah and Shrivastava; Kraiem*et al.*, 2021).

A. Encircling

The encircling process is the first step the wolf pack adopts in hunting down prey. The process involves the grey wolf pack encircling the prey which is analogous to the optimum solution. It is expressed mathematically as follows:

$$\vec{M} = |\vec{F}.\overrightarrow{X_p}(i) - \overrightarrow{X_w}(i) \quad (13)$$

$$\overrightarrow{X_w}(i+1) = \overrightarrow{X_p}(t) - \vec{N} * \vec{M} \quad (14)$$

Here i denotes the current iteration time step, $\vec{N}, \vec{M}$ and $\vec{F}$ are vector coefficients, $\overrightarrow{X_w}$ and $\overrightarrow{X_p}$represents the position vectors of wolf and prey respectively. The vector coefficients $\vec{M}$ and $\vec{N}$ are obtained as follows:

$$\vec{M} = 2\vec{a} * \overrightarrow{r_a} \ \ldots \quad (15)$$

$$\vec{N} = 2\overrightarrow{r_b} \ \ldots \quad (16)$$

Where values of the vector $\vec{a}$ is linearly decreased from 2 to 0 during the iteration while, $\overrightarrow{r_a}$and $\overrightarrow{r_b}$are random vectors ϵ[0, 1].

B. Hunting

Since the position of the optimum location is unknown unlike in a practical hunting scenario, the alpha, beta and delta solutions are used as a rough estimate since they are representatives of the top three best solutions respectively. Thus, the mean position of the alpha, beta and delta Wolfs were revealing of the prey's location as in (17). While in equations (18) the alpha, beta and delta Wolfs locations respectively are updated towards the prey's location which is indicative of the optimal solution.

$$\overrightarrow{X_p}(i+1) = (\overrightarrow{X_1} + \overrightarrow{X_2} + \overrightarrow{X_3})/3 \ldots \quad (17)$$

Where,

$$\begin{cases} \overrightarrow{X_1} = \overrightarrow{X_\alpha} - \vec{N}_1 * (\vec{M}_\alpha) \\ \overrightarrow{X_2} = \overrightarrow{X_\beta} - \vec{N}_1 * (\vec{M}_\beta) \\ \overrightarrow{X_2} = \overrightarrow{X_\delta} - \vec{N}_1 * (\vec{M}_\delta) \end{cases} \text{ and}$$

$$\begin{cases} \vec{M}_\alpha = |\vec{V}_\alpha \overrightarrow{X_\alpha} - \overrightarrow{X_w}| \\ \vec{M}_\beta = |\vec{V}_\beta \overrightarrow{X_\beta} - \overrightarrow{X_w}| \\ \vec{M}_\delta = |\vec{V}_\delta \overrightarrow{X_\delta} - \overrightarrow{X_w}| \end{cases} \ldots \quad (18)$$

C.Attacking

Practically, like the grey wolf inches close to the prey, its movement will become smaller and it will finally attack the prey. Similarly, in the GWO, the decreased movement of the grey wolf towards the prey is analogous to the simulated annealing of vector $\vec{a}$ from 2 to 0, as the optimal solution (prey) is approached. Figure 3, shows the GWO algorithmic flowchart.

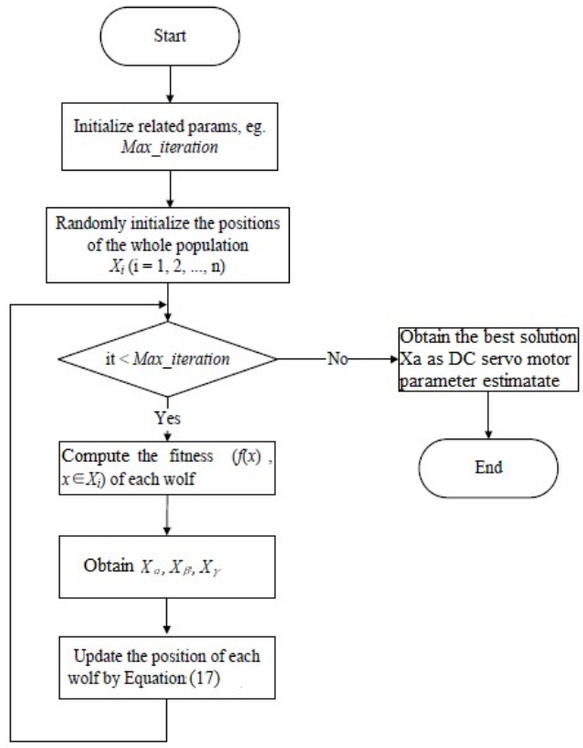

Figure 3: GWO algorithm flowchart (Pan et al. 2019)

2.3.2 Whale Optimization Algorithm

The whale optimisation algorithm (WOA) first proposed in(Mirjalili and Lewis, 2016) is a swarm intelligence meta-heuristic optimisation algorithm inspired by the bubble-net foraging social behaviour of humpback whales (Ning and Cao, 2021). The whale bubble-net foraging involves three stages; encircling prey, bubble-net attack and hunting prey.

A. Encircling prey

The humpback whales (search agent) see prey (solution) and encircle it. Nevertheless, since the optimum location of the solution is unknown, the current best candidate is substituted as the solution, while the other candidates update their information on the position towards the best candidate. The behaviour is defined mathematically as follows:

$$\vec{D} = |\vec{C} * \overrightarrow{\emptyset^*}(k) - \vec{\emptyset}(k)| \quad \ldots \quad (19)$$
$$\vec{\emptyset}(k+1) = \overrightarrow{\emptyset^*}(k) - \vec{A} * \vec{D} \ldots \quad (20)$$

Where k is the current iteration, $\vec{A}$ and $\vec{D}$ are vector coefficients, $\overrightarrow{\emptyset^*}(k)$ is the position vector of the current best candidate solution, $\vec{\emptyset}(k)$ is the position vector.
The vector coefficients $\vec{A}$ and $\vec{C}$ are obtained as follows:

$$\vec{A} = 2\vec{b} * \vec{r_c} - \vec{b} \ldots \quad (21)$$
$$\vec{C} = 2.\vec{r_d} \quad \ldots \quad (22)$$

Where, $\vec{r_c}$ and $\vec{r_d}$ are randomised vector coefficients [0,1] while, $\vec{b}$ is annealed from 2 to 0 during the iteration to allow exploration and exploitation respectively.

B. Bubble-net attack

The whale's feeding behaviour entails a constricted spiral movement towards the prey. Therefore, these two approaches; shrinking and surrounding are presented to explain this mechanism mathematically as follows:

$$\vec{\emptyset}(k+1) = \overrightarrow{D'} * e^{\gamma l} * \cos(2\pi l) + \overrightarrow{\emptyset^*}(k) \ldots \quad (23)$$

Where, $\overrightarrow{D'}$ is the variance between the n^{th}whale and the current optimal solution, γ is the constant value which defines the logarithmic spiral form or circular movement, and l is a randomised value [-1,1].

C. Hunting prey

In addition to the bubble-net foraging behaviour, the humpback whale can randomly search for prey. Thus, this behavioural dynamic is modelled as follows:

$$\overrightarrow{D'} = |\overrightarrow{\emptyset^*}(k) - \vec{\emptyset}(\mathrm{k})| \ldots \quad (24)$$
$$\overrightarrow{D'} = |\vec{C}\overrightarrow{\emptyset_r}(k) - \vec{\emptyset}(\mathrm{k})| \ldots (25)$$
$$\vec{\emptyset}(k+1) = \overrightarrow{\emptyset_r}(k) \text{-} \vec{A} * \vec{D} \ldots \quad (26)$$

Where, $\overrightarrow{\emptyset_r}(k)$ is the position of a random candidate.

Thus, the search agent's position is updated by a random agent if |A| > 1 and by the best solution if |A|< 1 this ensures exploration and exploitation respectively and the algorithm is terminated if the terminating criterion is satisfied. Figure 4, shows the Whale algorithm.

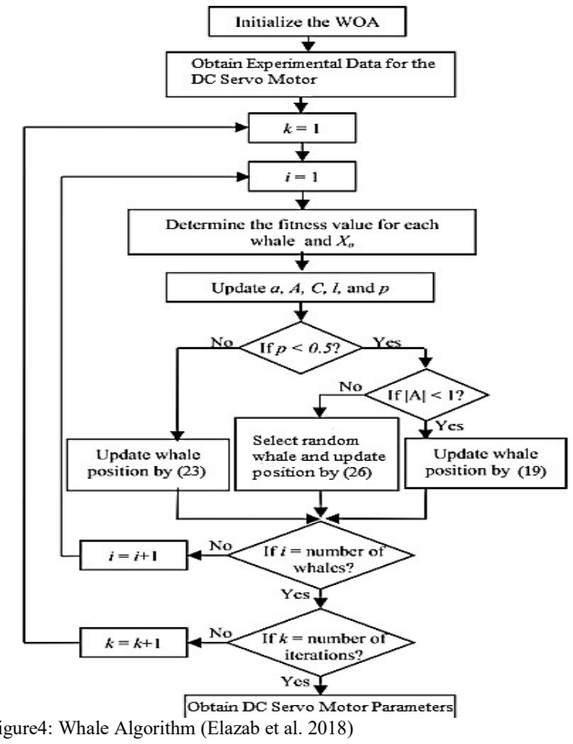

Figure4: Whale Algorithm (Elazab et al. 2018)

2.3.3 Genetic Algorithm

The Genetic Algorithm is an intelligent meta-heuristic optimization tool that mimics natural selection and genetics theory. Individuals forming a population exist in GA as a reasonable solution to a particular problem. Some merits of GA include its easy implementation and the fact that knowledge of plant traits is not necessary for the evaluation (fitness) function. It also works for non-linear systems and avoids convergence to local minima. GA consists of three major phases: selection, crossover, and mutation (Nyong-Bassey and Akinloye, 2014).

A. Selection Phase

El-Bakly (2009) used a roulette wheel to select individuals for the first generation, whereas Gadoue*et al*., (2009) use a stochastic uniform to select individuals for the first generation. Each iteration represents a generation in an iterative process. As a result, at the end of each generation, individuals are compared to an evaluation function and chosen for mating to produce new offspring. As specified in the algorithm, the offspring usually have the good traits of their progenitor and have evolved through some degree of mutation and crossover genetic process as specified in the algorithm Shuaib and Ahmed, (2014). The mathematical representation determines the population size for subsequent generations:

$$Number\ of\ offspring = P_s\ * relative\ fitness \ldots (27)$$

where, $P_s$is Population size.

B. Crossover Phase

The mating pairs after the selection phase undergo a crossover genetic procedure which is performed by crossover probability to give rise to new offspring with enhanced genetic traits. Mathematically, crossover operation is given as:

$$\tilde{P}_c = \alpha\tilde{P}_1 + (1-\lambda)\tilde{P}_2 \quad : \quad \tilde{P}_1 \neq \tilde{P}_2 \ldots (28)$$

Where, $\tilde{P}_1$ and $\tilde{P}_2$ are dissimilar parent chromosomes, α is a stochastically acquired natural number, $\lambda \in [0,1]$.

A small crossover value is usually selected for a large population size in other to enhance the individuals while retaining the best characteristics of both parents (Nyong-Bassey and Akinloye, 2014).

C. Mutation Phase

The mutation phase occurs after the crossover process mimicking the real-life process of mutation which involves the modification of the genome on rare occasions. Hence the occurrence of mutation is usually low for the preservation of good chromosomes. The objective of introducing mutation is to avoid convergence of local minima and increase the fitness of the individual as a possible solution by chromosome mutation. The authors (El-Bakly, 2009) suggested using the following formula to determine the mutation rate:

$$P_{mp} = \frac{1}{P_S\sqrt{L}} \ldots (29)$$

Where, P_{mp} is the finest mutation rate, P_s is the population size and L is the length of an individual random string. Figure 5, shows the GA algorithmic flowchart.

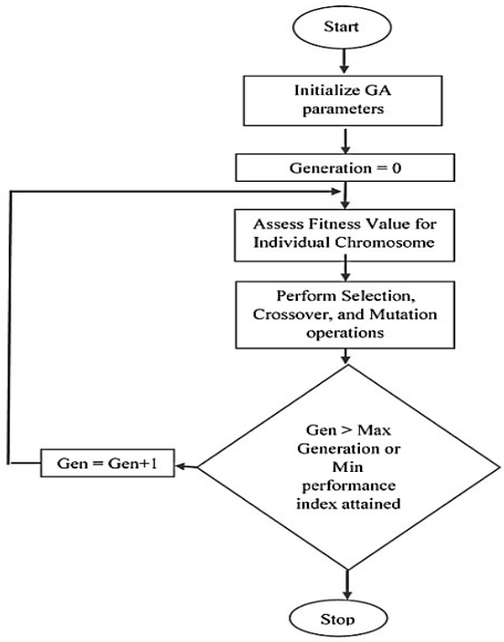

Figure 5: GA Flow Chart (Nyong-Bassey and Akinloye, 2016)

3. RESULTS AND DISCUSSIONS

3.1 Determination of Servo Motor Open-loop Speed Transfer function

The experimental setup was implemented based on Figure 6.To determine the servo gain constant *Km*, a 15V power supply is connected to the tachometer module GT150X. Also, 0 to 3V was applied to utilise the second socket of the AU150B to connect the first input of PA150C and the Servo amp SA150D.

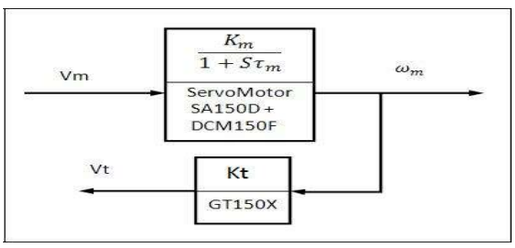

Figure6: SA150D+DCM150F+GT150X block diagram (Kabita, 2015)

Thereafter, the Servomechanism parameters are to be determined by observing the scope traces, and voltage readings and by performing arithmetic calculations as shown in Table 1a and Table 1b.

Table 1a: Experimental parameters of the DC servomotor.

Servomotor Input Voltage $V_m(V)$	Tachometer speed (n) (RPM)	Angular velocity ω (rad/sec)	Tacho-meter Voltage $V_t(V)$
1.00	3120	326.73	8.62
1.50	3150	329.87	8.64
2.00	3150	329.87	8.67
2.50	3150	329.87	8.69
-1.00	-3130	-327.77	-8.83
-1.50	-3150	-329.87	-8.83
-2.00	-3150	-329.87	-8.83
-2.50	-3150	-329.87	-8.83

Table 1b: Experimental calculated parameters for the DC servomotor

Servomotor Input Voltage $V_m(V)$	Tacho-meter Sensitivity $K_t = (\mathbf{Vt/\omega})$	Servo Gain $K_m = \boldsymbol{\omega}/\mathbf{Vm}$	Servo Gain $K_m = V_t/(V_m * K_t)$
1.000	0.026	272.27	272.27
1.500	0.026	219.91	219.91
2.000	0.026	164.93	164.93
2.500	0.026	131.95	131.95
-1.000	0.026	273.14	273.14
-1.500	0.026	219.91	219.91
-2.000	0.026	164.93	164.93
-2.500	0.026	131.95	131.95

To determine the time constant *Tm*, a function generator was used to generate a square wave voltage which served as the servomotor input voltage, *Vm* and had a frequency of 0.25Hz. The amplitude range of the square wave voltage was +/-1.0V and +/-2.0V while, the resulting Tachometer voltage, *Vt* and Time constant, *Tm*values were recorded accordingly as shown in Table 2.

Table 2: Time constant and tachometer voltage values captured from scope traces during anti/clockwise rotation

Square wave amplitude (Vm)	Tachometer Voltage (Vt)	Time Constant (T_m)	Angular velocity $\boldsymbol{\omega}$	Servo Gain $K_m = \boldsymbol{\omega}/\mathbf{Vm}$
1.0*V*	8.7 *V*	162 *mS*	329.87 rad/sec	272.27
2.0 *V*	8.7 *V*	162 *mS*	329.87 rad/sec	164.93
-1.0V	-8.7V	162mS	-329.87 rad/sec	272.27
-2.0V	-8.7V	162mS	-329.87 rad/sec	164.93

Therefore, the average time constant values in Tables II, which resulted from the output response curve for the forward and reverse motoring as displayed on the scope was 162mS. Thus, the speed open loop T.F of the Servo motor is:

$$G(s) = 272.27/(0.162s + 1) \quad (30)$$

The experimental open-loop speed step response of the Servomechanism and angular speed versus voltage are shown in Figure7.

Therefore, since the servo-gear mechanism's transfer function H(s) is known, the open-loop position transfer function is as follows:

$$T(s) = G(s) * H(s) \quad (31)$$

Therefore, the open-loop position T.F is expressed as:

$$T(s) = 272.27 * 6.61/(0.162s + 1)s \quad (32)$$

And the closed-loop position with velocity feedback T.F:

$$T(s) = 1800/(0.162s^2 + 273.27s + 1800) \quad (33)$$

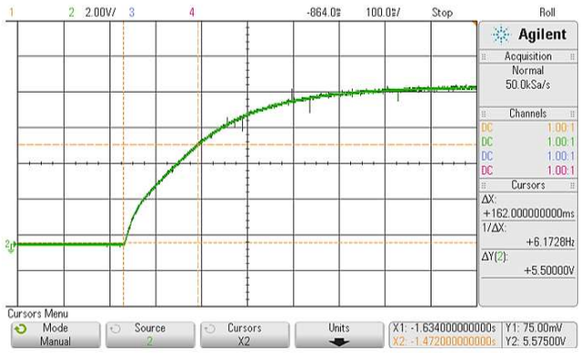

Figure7: Experimental open-loop speed step response of the Servo motor

3.2 Comparison of Meta-heuristic optimisation algorithms

The closed-loop position with velocity feedback transfer function which is obtained from the experimental open-loop speed step response of the servomechanism is simulated in MATLAB. Thereafter, the meta-heuristic optimisation algorithms WOA, GWO and GA were independently deployed to estimate the servomechanism electrical and mechanical parameters. To perform the parameter estimation using the algorithms, a fitness function is used to iteratively minimises the mean squared error between the experimental step response data and the corresponding step response generated by the optimisation algorithm. Thus, the corresponding fitness function scores for WOA, GWO and GA were 1.09351, 1.90374 and 0.000706 as presented in Figures 8, 9 and 10 (a) respectively, with Figures 10 (b) - (d) consequently, showing the best individuals, individuals in a generation and the fitness score ranges for the GA.

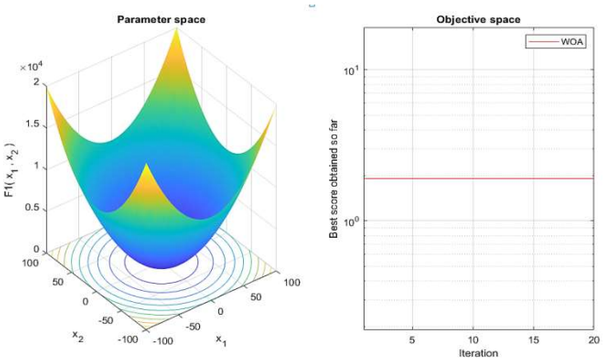

Figure 8: Closed-loop position step response fitness score with a velocity feedback loop with the WOA method

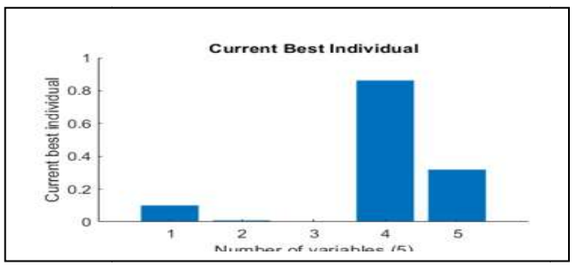

Figure10 (b): Best Individual for GA method

Figure 10 (c): Individual per generation for the GA method

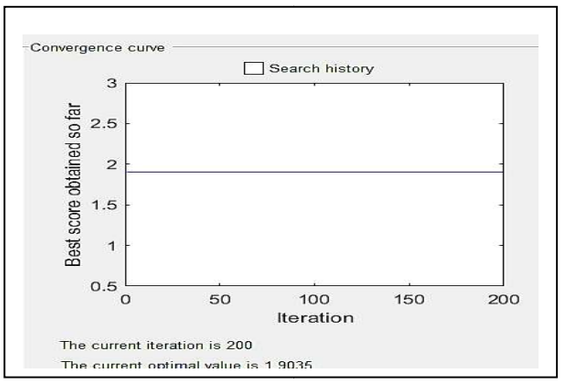

Figure9: Closed-loop position step response fitness score with a velocity feedback loop with GWO method

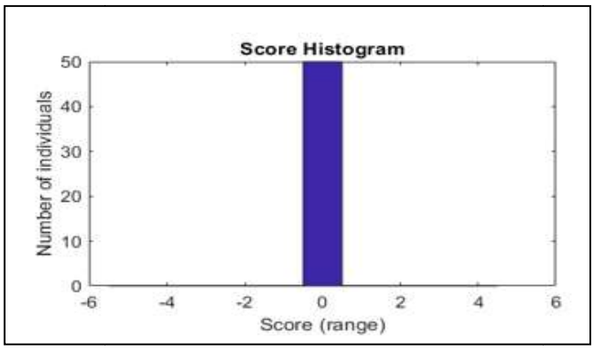

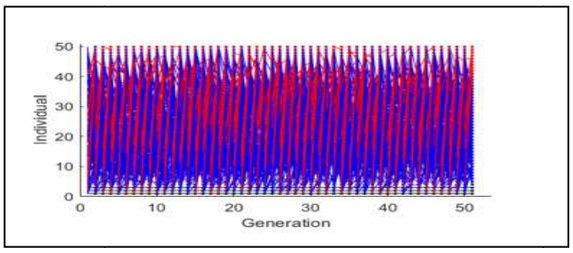

Figure 10 (d): Score range for individuals with a GA algorithm

Figure 10 (a): Closed-loop position step response fitness score with a velocity feedback loop with GA method

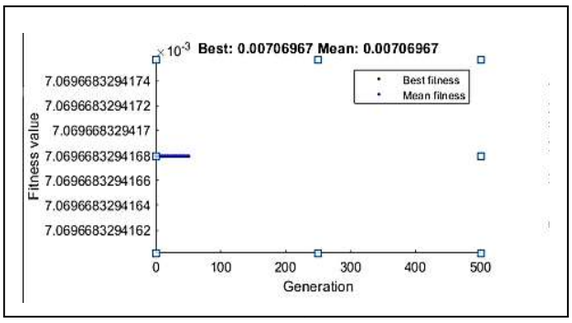

Hence, the GA has the best fitness score, while the WOA was only negligibly better than GWO.

Furthermore, as seen in Figure 11, the transient characteristics of the position close loop with velocity feedback step response of the estimated servomechanism with GA closely match that of the experiment. In Fig. 8, the experimental benchmark step response had a rise time of 0.33s i.e., the response marked up from 10% reaches 90% of the steady-state value of 1 radian. While the GA had the

fastest rise time which took 1.2s compared to the experimental step response, the GWO had the second-best rise time of 17.9s which was closely followed by WOA which had the slowest rise time of 21.3s. Similarly, the experimental step response had a settling time of 0.59s which was closely followed by the GA with 2.18s. The GWO which had a settling time of 31.9s was only better than the WOA which had 37.9s. Table 3, summarises the results of estimated parameters of the servomechanism and RMSE fitness score for the meta-heuristic algorithms. The generic pseudo-code for the DC parameter estimation using GA, GWO and WOA have been presented in Table 4.

Figure 11: Position closed-loop step response with velocity feedback for the estimated Servomechanism.

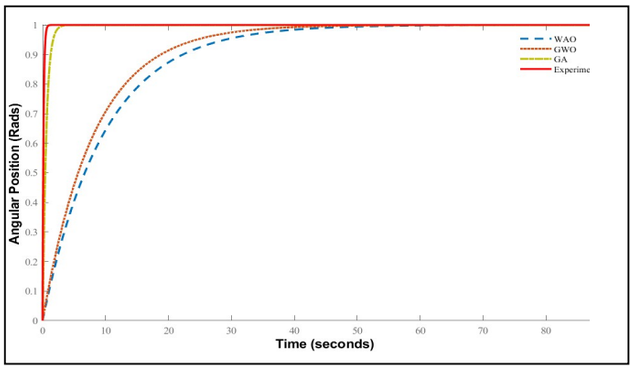

Table 3: Estimated Servo Motor parameters and Performance index

Motor Parameters Value	WOA	GWO	GA
Mechanical damping (Friction) factor 'B' in *Nms*	0.024	0.01517	0.1
Moment of inertia for motor rotor 'J' in $Kg.m^2$	0.00082	0.00046278	0.009
Inductance of the armature 'L' in *H*	0.01	0.01	1e-6
Resistance of the armature 'R' in Ω	11.9	9.5317	0.862
Back E.M.F constant 'K' in *Nm/A*	9.65	8.1422	0.319
RMSE Fitness Score	1.90374	1.90351	0.00706

Table 4: Generic Pseudo Code for Parameter Estimation using GWO, WOA and GA.

1	Initialise the optimisation i.e., GWO or GA or WOA.
2	Specify the initialization parameters such as fitness function, iteration, number of particles for GWO and WOA or population size and number of generations GA.
3	Run the GWO or WOA or GA optimisation algorithm using initial guess parameter values.
4	Compare the fitness score of the Model output to the Experimental Data.
5	(a) If GA is activated,select parents and reproduce offspring generation using crossover with 5% mutation. (b) If GWO is activated or selected; i. Update all the individual search agents (grey wolfs) based on the average position of the agents, then update a, A and C. ii. Update the Alpha, beta and delta wolf positions. (c) If WOA is activated by equal probability of h<0.5 i. if |A|< 1, update the agents (Whales) in the ocean with the fittest whale ii. If |A|>1, update the whales based on the position of a random whale. Else If h>0.5 update the whales based on equation
6	Repeat 4 and 5 until iteration or number of generation criteria are exceeded.
7	Return optimised estimated parameters for the DC Servo motor (i.e., represented by the Alpha Grey wolf in GWO, fittest individual and Whale in GA and WOA respectively).
8	End

4. CONCLUSION

The paper dealt with Servomechanism parameter system identification using the time domain response and meta-heuristic algorithms. Firstly, to determine the position closed-loop transfer function of the servomechanism for parameterisation, the first order speed response transfer function parameters; time constant and DC gain of the servomechanism were investigated experimentally. The servo gain which was determined for a range of input voltages showed an inverse relationship. The time constant determined as 162ms was found to be the same in both forward and reverse rotation. Thus, the step response method was used to identify the servo time system parameters for the open-loop speed and position response. Thereafter, the meta-heuristic algorithms were compared to the simulated closed-loop transfer function and the experimental step response of the servomechanism.

Investigating the parameters of the servomechanism, GA resulted in the least RMSE fitness score of 0.00706 in contrast with the GWO and WOA which had a score of 1.90351 and 1.90374 respectively. Therefore, the parameters obtained using the GA method depicted the most practical and realistic agreement with the experimental position (velocity feedback) closed-loop step response of the servo mechanism.

REFERENCES

Abokhatwa, S., and Said, O. (2019). DC Motor Parameter Identification Using Speed Step Response, 2nd Conference for Engineering Sciences and Technology CEST2, 29 – 31 October 2019, Sabratha, Libya.

Adewusi, S. (2016). Modelling and parameter identification of a DC motor using constraint optimization technique. IOSR Journal of Mechanical and Civil Engineering (IOSR-JMCE), Vol. 13 No. 6: pp. 46-56.

Armstrong M. (2015). EEE 8007 Advanced Control System Notes, Newcastle University.

Bartelt, T. L. (2010). Industrial Automated Systems: Instrumentation and Motion Control. Cengage Learning.

Chun, S., and Kim, T. H. (2018). Simultaneous identification of model structure and the associated parameters for linear systems based on particle swarm optimization. Complexity, 2018.

Elazab, O. S., Hasanien, H. M., Elgendy, M. A., and Abdeen, A. M. (2018). Parameters estimation of single-and multiple-diode photovoltaic model using whale optimisation algorithm. *IET Renewable Power Generation*, *12*(15), 1755-1761.

El-Bakly, A., Fouda, A., and Sabry, W. (2009). A proposed DC motor sliding mode position controller design using fuzzy logic and PID techniques, In International Conference on Aerospace Sciences and Aviation Technology. Cairo, Egypt. Vol. 13, pp. 1-9.

Fang, C., Jin, Z., Wu, J., and Liu, C. (2021). Estimation of Lithium-Ion Battery SOC Model Based on AGA-FOUKF Algorithm. Frontiers in energy research, Vol 9.

Feedback Instruments, Modular Servo Instructional System MS150, available at http://www.feedback-instruments.com/pdf/brochures/MS150_Datasheet_Modular_Servo_System_10_2013.pdf [accessed 03/01/2022].

Fuh, C. C., and Tsai, H. H. (2007). Adaptive parameter identification of servo control systems with noise and high-frequency uncertainties. Mechanical Systems and Signal Processing, Vol 21 No. 3: pp. 1437-1451.

Gadoue, S. M., Giaouris, D., and Finch, J. W. (2009). Artificial intelligence-based speed control of DTC induction motor drives—A comparative study. Electric Power Systems Research, Vol. 79 No.

1: pp. 210-219.

Garrido, R. and Concha, A., (2010). Combining Algebraic Identification and a Least Squares method for DC servomechanism identification. In: Electrical Engineering Computing Science and Automatic Control (CCE), 7th International Conference.Tuxtla Gutierrez, Mexico. pp. 28-33.

Garrido, R., and Miranda, R. (2012). DC servomechanism parameter identification: A closed-loop input error approach. ISA transactions, Vol 51 No. 1: pp. 42-49.

Guo, Q., Gao, L., Chu, X., and Sun, H. (2022). Parameter identification of static var compensator model using sensitivity analysis and improved whale optimization algorithm. CSEE Journal of Power and Energy Systems.

Kabita A. (2015). EEE 8074 Servomechanism and Systems Identification Laboratory Notes, Newcastle University.

Kim, M.S. and Chung, S.C., (2003). Identification of nonlinear characteristics for precision servomechanisms. In: Proceedings of the ASPE 2003 Annual Meeting, Raleigh, USA. pp. 167-170.

Kraiem, H., Aymen, F., Yahya, L., Triviño, A., Alharthi, M., and Ghoneim, S. S. (2021). A comparison between particle swarm and grey wolf optimization algorithms for improving the battery autonomy in a photovoltaic system. Applied Sciences, Vol. 11 No. 16: pp. 7732.

Kushwah, Y. S., and Shrivastava, R. (2018). Particle Swarm Optimization (PSO) Inspired Grey Wolf Optimization (GWO) Algorithm. Int. J. Math. Trends Technol., Vol. 58 No. 2: pp. 135-149.

Mirjalili, S., Mirjalili, S. M., and Lewis, A. (2014). Grey wolf optimizer. Advances in engineering software, Vol. 69: pp. 46-61.

Mirjalili, S., and Lewis, A. (2016). The whale optimization algorithm. Advances in engineering software, Vol. 95: pp. 51-67.

Mohamed, O. A., Okasha, A., and Abdrabbo, S. (2018). Online Identification and Artificial Intelligence Control of a Servo Pneumatic System. Scientific Journal, Vol 4 No. 2: pp. 60-74.

Nadweh, S., Khaddam, O., Hayek, G., Atieh, B., and Alhelou, H. H. (2020). Steady-state analysis of modern industrial variable speed drive systems using controllers adjusted via grey wolf algorithm & particle swarm optimization. Heliyon, Vol. 6 No. 11: pp. 1-9.

Nayak, B., & Sahu, S. (2019). Parameter estimation of DC motor through whale optimization algorithm. International Journal of Power Electronics and Drive Systems, Vol. 10 No. 1: pp. 83-92.

Ning, G. Y., and Cao, D. Q. (2021). Improved whale optimization algorithm for solving constrained optimization problems. Discrete Dynamics in Nature and Society, Vol. 2021: pp. 1-13.

Nyong-Bassey, B. E., and Akinloye, B. (2014). Comparative study of optimised artificial intelligence-based first order sliding mode controllers for position control of a DC motor actuator. Journal of Automation, Mobile Robotics and Intelligent Systems, Vol. 10 No. 3: pp. 58-71.

Pan, J. S., Hu, P., & Chu, S. C. (2019). Novel parallel heterogeneous meta-heuristic and its communication strategies for the prediction of wind power. *Processes*, *7*(11), 845.

Pan, Y., Liu, X., Zhu, Y., Liu, B., and Li, Z. (2021). Feedforward Decoupling Control of Interior Permanent Magnet Synchronous Motor with Genetic Algorithm Parameter Identification. Progress In Electromagnetics Research, Vol 102: pp. 117-126.

Rezazade, A. R. (2010). GA-based servo system parameter estimation during startup. International Journal of Engineering and Applied Sciences, Vol. 2 No. 2: pp. 33-43.

Shuaib, A. O., and Ahmed, M. M. (2014). Robust PID control system design using ITAE performance index (DC motor model). International Journal of Innovative Research in Science, Engineering and Technology, Vol. 3 No. 8: pp. 15060-15067.

Throne, R. (2005). Frequency domain system identification of one, two, and three degrees of freedom systems in an introductory controls class. In: Proceedings of the 2005 American Society for Engineering Education Annual Conference and Exposition, Texas, USA, pp. 10-643.

Wang, J. S., & Li, S. X. (2019). An improved grey wolf optimizer based on differential evolution and elimination mechanism. Scientific reports, Vol. 9 No. 1: pp. 1-21.

Wu, Z., Yang, R., Guo, C., Ge, S., and Chen, X. (2019). Analysis and Verification of Finite Time Servo System Control with PSO Identification for Electric Servo System. Energies, Vol. 12 No. 18: pp. 3578.

Wu, Z., Wang, G., Xie, Z., He, Y., and Lu, X. (2020). Lithium battery SOC estimation based on whale optimization algorithm and unscented Kalman filter. Journal of Renewable and Sustainable Energy, Vol. 12 No. 6: pp. 1-7.